Ghrelin alleviates paclitaxel-induced peripheral neuropathy by reducing oxidative stress and enhancing mitochondrial anti-oxidant functions in mice

Nobuyuki Ishii [a], Hironobu Tsubouchi [a,*], Ayako Miura [a], Shigehisa Yanagi [a], Hiroaki Ueno [a], Kazutaka Shiomi [a], Masamitsu Nakazato [a]

[a] Division of Neurology, Respirology, Endocrinology and Metabolism, Department of Internal Medicine, Faculty of Medicine, University of Miyazaki, Miyazaki, Japan

[*] Corresponding author: Hironobu Tsubouchi

Division of Neurology, Respirology, Endocrinology and Metabolism, Department of Internal Medicine, University of Miyazaki, 5200 Kihara, Kiyotake, Miyazaki, 889-1692, Japan

Tel: +81-985-85-2965 Fax: +81-985-85-1869

E-mail address: hironobu_tsubouchi@med.miyazaki-u.ac.jp

Abstract

Paclitaxel is an effective chemotherapeutic agent, but has some treatment-limiting adverse effects that markedly decrease patients' quality of life. Peripheral neuropathy is one of these, and no treatment for it has been established yet. Ghrelin, an endogenous ligand for the growth hormone secretagogue receptor, is secreted from the stomach and has widespread effects on multiple systems. We investigated the pharmacological potential of ghrelin in preventing paclitaxel-induced peripheral neuropathy using wild-type mice, ghrelin-null mice, and growth hormone secretagogue receptor-null mice. In wild-type mice, ghrelin administration alleviated mechanical and thermal hypersensitivity, and partially prevented neuronal loss of small unmyelinated intraepidermal nerve fibers but not large myelinated nerve fibers. Moreover, ghrelin administration decreased plasma oxidative and nitrosative stress and increased the expression of uncoupling protein 2 (UCP2) and superoxide dismutase 2 (SOD2) in the dorsal root ganglia, which are mitochondrial antioxidant proteins, and peroxisome proliferator-activated receptor gamma coactivator 1-alpha (PGC-1α), a regulator of mitochondrial number. Both ghrelin-null mice and growth hormone secretagogue receptor-null mice developed more severe nerve injuries than wild-type mice. Our results suggest that ghrelin administration exerts a protective effect against paclitaxel-induced neuropathy by reducing oxidative stress and enhancing mitochondrial anti-oxidant functions, and that endogenous ghrelin has a

neuroprotective effect that is mediated by ghrelin/growth hormone secretagogue receptor signaling. Ghrelin could be a promising therapeutic agent for the management of this intractable disease.

Keywords

Ghrelin, Growth hormone secretagogue receptor, Paclitaxel, Chemotherapy-induced peripheral neuropathy, Peripheral neuropathic pain, PC12

1. Introduction

Paclitaxel is a taxane-derived anti-neoplastic agent that is commonly used for solid tumors such as ovarian, breast, and lung cancers. It is highly effective against these cancers but has several treatment-limiting adverse effects (reviewed in (Rowinsky and Donehower, 1995)). Clinical symptoms of paclitaxel-induced peripheral neuropathy include numbness, tingling, and burning pain in a glove-and-stocking distribution, leading to markedly decreased quality of life (Tofthagen, 2010). However, prophylactic therapies for paclitaxel-induced neuropathy have not been established thus far.

Ghrelin, an endogenous ligand for the growth hormone secretagogue receptor, is secreted from the stomach. It acts on the pituitary to stimulate growth hormone release, and on the hypothalamus to enhance food intake (Kojima et al., 1999; Nakazato et al., 2001). Ghrelin also has widespread effects on multiple systems, influencing glucose metabolism, cell proliferation, and gastrointestinal, cardiovascular, and immune function (reviewed in (Kojima and Kangawa, 2006)). In addition, ghrelin has been reported to exert a neuroprotective effect on the peripheral nervous system against conditions such as diabetic neuropathy (Kyoraku et al., 2009; Tsuchimochi et al., 2013) and cisplatin-induced peripheral neuropathy (Garcia et al., 2008). However, it remains unclear whether ghrelin attenuates paclitaxel-induced neuropathy

and which portions of the peripheral neurons it protects. Moreover, the mechanism by which ghrelin exerts a neuroprotective effect on the peripheral nervous system is unclear.

In this study, we examined ghrelin's effects in a murine model of paclitaxel-induced peripheral neuropathy, focusing on histology and neuroprotective mechanisms in the peripheral nerves. We further investigated the neuroprotective effect of the endogenous ghrelin/growth hormone secretagogue receptor system using ghrelin-null and growth hormone secretagogue receptor-null mice.

2. Methods and materials

2.1. Animals

Male 8- to 10-week-old C57BL/6J mice (wild-type [WT] mice) were purchased from Charles River Japan (Yokohama, Japan). Eight-week-old ghrelin-null (Sato et al., 2008) and growth hormone secretagogue receptor-null mice (Sun et al., 2004) were generously provided by Dr. M. Kojima (Kurume University, Fukuoka, Japan) and Dr. R. G. Smith (Baylor College of Medicine, Houston, TX), respectively. Growth hormone secretagogue receptor-enhanced green fluorescent protein (eGFP) reporter mice were obtained from Mutant Mouse Resource & Research Centers at University of California, Davis. All mice were housed under controlled temperature (21–23°C) on a 12-h light (08:00—20:00)/12-h dark cycle, and fed standard laboratory chow with ad libitum access to food. All experimental procedures were approved by the Animal Care and Use Committee of the University of Miyazaki.

2.2. Administration of paclitaxel and ghrelin

Paclitaxel 2 mg/kg (Nippon Kayaku, Tokyo, Japan) or vehicle (Cremophor EL and 99.9% ethanol at a 1:1 ratio) were administered to mice intraperitoneally (i.p.), in a volume of 0.2 ml, once per day for 5 consecutive days (cumulative dose of 10 mg/kg) (Masocha, 2014). Concurrently with paclitaxel or vehicle administration, 300 nmol/kg/0.2 ml ghrelin or 0.2 ml

PBS were intraperitoneally injected into the mice once per day for 5 consecutive days. This ghrelin administration protocol was modified from that of our previous work (Kyoraku et al., 2009; Tsuchimochi et al., 2013). WT mice were divided into three groups: “control” (vehicle + PBS), “PTX + PBS” (paclitaxel + PBS), and “PTX + ghrelin” (paclitaxel + ghrelin). Ghrelin-null and growth hormone secretagogue receptor-null mice were injected with paclitaxel 2 mg/kg and PBS for 5 consecutive days. Body weights and behavioral analyses were evaluated on day 1 before drug administration and on day 7. In addition, histological analysis, measurement of oxidative and nitrosative stress, and quantitative PCR were conducted after mice were euthanized on day 7.

2.3. Cell culture and administration of paclitaxel and ghrelin

Rat pheochromocytoma PC12 cells were obtained from the RIKEN Cell Bank (Ibaraki, Japan), and maintained in Dulbecco's modified Eagle's medium (DMEM) supplemented with 10% fetal bovine serum, 10% horse serum, and 1% penicillin-streptomycin at 37°C in humidified 5% CO_2. These cells were exposed to paclitaxel (1 μM) in the presence or absence of ghrelin (10 μM) for 24 h, as described previously (Liu et al., 2013; Konaka et al., 2017), followed by immunocytochemistry and western blotting.

2.4. Behavioral analyses

Mechanical and thermal sensitivities were measured on day 1 before paclitaxel administration and on day 7. Mechanical sensitivity was assessed by measuring the 50% mechanical withdrawal threshold with calibrated von Frey filaments (Muromachi Kikai, Tokyo, Japan) using the up–down method (Chaplan et al., 1994; Sommer and Schafers, 1998). Briefly, mice were placed in plastic cages with an elevated wire mesh floor, and allowed to acclimate for 15 min before testing. Increasing strengths (0.4–8.0 gram) of von Frey filaments were applied sequentially to the plantar surface of the hind paw of each mouse. The strength of the filament that caused paw withdrawal in 3 of the 6 applications was defined as the 50% mechanical withdrawal threshold.

Thermal sensitivity was evaluated by measuring the thermal withdrawal threshold using the hot plate test, as described previously (Kyoraku et al., 2009; Tsuchimochi et al., 2013; Masocha et al., 2016). Briefly, mice were placed on a hot plate (Muromachi Kikai, Tokyo, Japan) with the temperature maintained at 55±1 °C after a 15-min acclimation period. The response latency to either a hind paw lick or to a jump was recorded. A cut-off time of 20 s was chosen to prevent tissue damage.

2.5. Immunohistochemistry

Mice were anesthetized by a mixed anesthetic agent (0.4 mg/kg of medetomidine, 2.0 mg/kg of midazolam, and 2.5 mg/kg of butorphanol) (Kawai et al., 2011) and transcardially perfused with ice-cold PBS followed by 4% PFA solution. Lumbar dorsal root ganglia and hind paw footpads were immersed in 4% paraformaldehyde/PBS overnight at 4°C, and subsequently cryoprotected in 0.1 M phosphate buffer (PB) containing 20% sucrose. The dorsal root ganglia and footpads were embedded in Tissue-Tek OCT compound (Sakura Finetek Japan, Tokyo, Japan) and were cut into 8-μm slide sections and 30-μm free-floating sections, respectively, using a cryostat (Leica CM3050S; Leica, Nussloch, Germany).

Dorsal root ganglia sections were blocked in Serum-Free Protein Block (Dako, Carpinteria, CA) for 10 min, and then incubated overnight at 4°C with rabbit anti-activating transcription factor 3 (ATF3) (1:500; Santa Cruz Biotechnology, Dallas, TX), a neuronal injury marker (Tsujino et al., 2000), and Alexa Fluor 488–conjugated mouse monoclonal anti-neuron specific nuclear protein (NeuN) (1:500; Merck Millipore, Billerica, MA), a neuronal marker to confirm that dorsal root ganglia sections actually contain neurons.

Footpad sections were incubated in blocking solution (0.01 M PBS containing 5% normal donkey serum, 2% bovine serum albumin, and 0.25% Triton X-100) for 1 h, then incubated overnight at 4°C with rabbit anti-protein gene product 9.5 (PGP9.5) (1:2000; Abcam, Cambridge, UK).

147 Both dorsal root ganglia and footpad sections were treated with Alexa Fluor 594–
148 labeled anti-rabbit secondary antibody (1:500; Invitrogen, Carlsbad, CA).
149 For quantification, 4 dorsal root ganglia sections per animal were randomly selected,
150 and ATF3- or NeuN-positive cells in these sections were examined with a Confocal Microscope
151 C2 (Nikon, Tokyo, Japan). The number of ATF3-positive cells was expressed as the percentage
152 of the number of NeuN-positive cells. Intraepidermal nerve fibers were quantified by the
153 method described previously (Ko et al., 2002). Briefly, nerve fibers crossing the basement
154 membrane were counted as one. The density was determined as the number of nerve fibers per
155 epidermal length.
156
157 *2.6. Immunocytochemistry*
158 After the plated PC12 cells were washed with PBS, they were fixed in 4%
159 paraformaldehyde in 0.1 M PBS for 20 min. The cells were blocked with Serum-Free Protein
160 Block (Dako, Carpinteria, CA) for 10 min, then incubated overnight at 4°C with rabbit anti-
161 superoxide dismutase 2 (SOD2) (1:500; Cell Signaling Technology, Danvers, MA). The cells
162 were treated with Alexa Fluor 488–labeled anti-rabbit secondary antibody (1:500; Invitrogen,
163 Carlsbad, CA). The sections were counterstained with 4’-6-diamidino-2-phenylindole (DAPI;
164 Dojindo, Kumamoto, Japan). Images were obtained with a Confocal Microscope C2 (Nikon,

Tokyo, Japan). The quantification method was developed using ImageJ software (National Institutes of Health, Bethesda, MD), and involved assigning a value for green fluorescence intensity to every pixel in a cell area, and calculating the average fluorescence intensity in eight cells across each slide.

2.7. Morphometry of sciatic nerves

The sciatic nerves were dissected, postfixed in 3% glutaraldehyde, osmicated in 1% osmium tetroxide, dehydrated, and embedded in epoxide resin. The embedded nerves were cut into 1-μm sections, which were stained with toluidine blue. The sections were examined with an OLYMPUS AX-7 fluorescence microscope (Olympus, Tokyo, Japan). Only the axons surrounded by myelin were counted. Morphometrical analysis was performed with the NIH ImageJ software (National Institutes of Health).

2.8. Extraction of mRNA and quantitative real-time PCR

The dorsal root ganglia were dissected on day 7, preserved in RNA-later (Ambion, Austin, TX), and stored at 20 °C until the analysis. RNA isolation was performed using the RiboPure Kit (Ambion, Austin, TX). First-strand cDNA was generated by reverse transcription using a High-Capacity RNA-to-cDNA Kit (Life Technologies Japan). Quantitative real-time

PCR was performed using TaqMan Fast Universal PCR Master Mix (Life Technologies Japan, Tokyo, Japan) and a Thermal Cycler Dice Real Time System II (Takara Bio, Kusatsu, Japan). The levels of mRNA were determined using cataloged primes (Applied Biosystems, Foster City, CA) for mice (uncoupling protein 2 [*Ucp2*], Mm00627599_m1; peroxisome proliferator-activated receptor gamma coactivator 1-alpha [*Pgc-1α*], Mm01208835_m1; *Sod2*, Mm01313000_m1; glyceraldehyde 3-phosphate dehydrogenase [*Gapdh*], Mm99999915_g1). UCP2 and PGC-1α are regulators of mitochondrial reactive oxygen species production (Andrews et al., 2005) and of mitochondrial number, respectively, and SOD2 is a key mitochondrial antioxidant enzyme. Expression of these genes was normalized to the expression of *Gapdh* mRNA, and the results were expressed as relative fold change.

2.9. Western blotting

Cytoplasmic and nuclear proteins were extracted from whole cells by RIPA buffer (Nacalai Tesque, Kyoto, Japan), and the extracts were transferred to a new prechilled tube and stored at -80°C until used. The protein contents of the extracts were determined by a Bradford assay. Equal amounts of proteins were fractionated by 10% SDS-PAGE and transferred to Immobilon-P Transfer Membranes (Merck Millipore). After blocking with 5% skimmed milk dissolved in 20 mM Tris–HCl buffer (pH 7.5) containing 137 mM NaCl and 0.05% Tween 20

for 1 h, the membrane was incubated with rabbit antibodies to SOD2 (1:5000; Cell Signaling Technology) or β-actin (1:5000; Sigma-Aldrich, St. Louis, MO) overnight at 4°C, followed by incubation with an anti-rabbit IgG antibody (1:2500; Cell Signaling Technology) conjugated with peroxidase. Proteins reactive to these antibodies were individually detected by the enhanced chemiluminescence method using an Immunostar Reagent (Wako, Osaka, Japan) and a Lumino image analyzer (LAS-1000; Fujifilm, Japan). To quantify protein expression, we used densitometry with ImageJ software on the lanes.

2.10 Oxidative and nitrosative stress measurements

At the end of the experiments, blood was obtained for the assessment of oxidative and nitrosative stress, as described previously (Tsuchimochi et al., 2013; Giuliani et al., 2014). Concentrations of 8-isoprostane and malondialdehyde, used as markers of lipid peroxidation, were measured with an 8-isoprostane EIA kit (Cayman Chemical, Ann Arbor, MI) and a colorimetric commercial kit (Sigma-Aldrich), respectively. The concentration of nitric oxide was also measured with a colorimetric commercial kit (Enzo Life Sciences, Farmingdale, NY).

2.11. Statistical analysis

Data are expressed as means ± standard error of the mean (S.E.M.). Differences

among multiple groups were determined via one-way analysis of variance (ANOVA) with Dunnett's post-hoc t-tests. When 2 mean values were compared, the analysis was performed with an unpaired *t*-test. *P*-values less than 0.05 were considered statistically significant.

3. Results

3.1. Ghrelin administration ameliorated paclitaxel-induced sensory disturbance

The PTX+PBS group showed decreases in both mechanical (Fig. 1A) and thermal (Fig. 1B) withdrawal thresholds on day 7 compared with the control group. These thresholds were significantly increased when ghrelin was administered concurrently with paclitaxel (PTX+ghrelin group).

3.2 Drug administration did not change mouse body weight

In the experimental protocol, the body weights of mice on day 7 were no different in the presence or absence of paclitaxel or ghrelin administration (Fig. 1C).

3.3. Growth hormone secretagogue receptor located in peripheral neurons in dorsal root ganglia

Immunohistochemistry with anti-GFP antibody revealed that growth hormone secretagogue receptor was expressed in dorsal root ganglia neurons in growth hormone secretagogue receptor-eGFP mice (Fig. 1D).

3.4. Ghrelin administration prevented paclitaxel-induced injuries of intraepidermal nerve fibers rather than large and myelinated nerve fibers

To assess the extent of neuronal injury in peripheral nerves, we examined the expression of ATF3 in lumbar dorsal root ganglia by immunohistochemistry. At day 7, the number of ATF3-positive neurons in the PTX+PBS group was significantly higher than that in the control group, while ghrelin administration significantly suppressed ATF3 expression compared with the PTX+PBS group (Fig. 2A, B). We morphologically evaluated the sciatic nerve and intraepidermal nerve fibers. The number of myelinated fibers in the sciatic nerve was not significantly different between the 3 groups (Fig. 2C, D). In the PTX+PBS group there were significantly fewer intraepidermal nerve fibers, and ghrelin administration prevented their loss (Fig. 2E, F).

3.5. Ghrelin administration reduced paclitaxel-induced oxidative and nitrosative stress, and increased mRNA expression levels of Ucp2, Pgc-1α, and Sod2 in the dorsal root ganglia

The plasma levels of 8-isoprostane, malondialdehyde, and nitric oxide were increased in paclitaxel-treated mice, and ghrelin significantly decreased these values (Fig. 3A–C). Ghrelin administration also increased the mRNA expression levels of *Ucp2*, *Pgc-1α*, and *Sod2* in the PTX+ghrelin group compared with the PTX+PBS group (Fig. 3D).

3.6. Ghrelin administration increased protein levels of SOD2 in paclitaxel-exposed PC12 cells

Immunocytochemistry with anti-SOD2 antibody and western blotting demonstrated that ghrelin significantly increased the protein level of SOD2 in paclitaxel-exposed PC12 cells compared with paclitaxel-exposed PC12 cells without ghrelin treatment (Fig. 3E, F).

3.7. Paclitaxel-induced peripheral nerve injuries were more severe in both ghrelin-null and growth hormone secretagogue receptor -null mice

On day 7, both ghrelin-null and growth hormone secretagogue receptor-null mice developed intense mechanical hypersensitivity following paclitaxel administration (Fig. 4A). In addition, both types of null mice demonstrated significant increases in the expression levels of ATF3 in their dorsal root ganglia compared with WT mice (Fig. 4B).

4. Discussion

In this study we demonstrated that ghrelin administration ameliorated experimental paclitaxel-induced neuropathy by preventing loss of intraepidermal nerve fibers. We suggest that ghrelin maintained mitochondrial function by increasing mitochondrial number and suppressing mitochondrial reactive oxygen species production, leading to decreased oxidative stress and to prevention of nerve injuries. In addition, we showed that endogenous ghrelin exerted a neuroprotective effect through ghrelin/ growth hormone secretagogue receptor signaling.

In rodent models of paclitaxel-induced neuropathic pain, sensory disturbances are caused by intraepidermal nerve fiber injuries, and are improved by preventing loss of intraepidermal nerve fibers (Boyette-Davis et al., 2011; Zhang et al., 2013; Ko et al., 2014; Zhang et al., 2016). Myelinated large fibers are much less impaired than intraepidermal nerve fibers in the paclitaxel-induced neuropathic pain model (Polomano et al., 2001; Bobylev et al., 2015). Ghrelin's neuroprotective effects have already been demonstrated in diabetic peripheral neuropathy (Kyoraku et al., 2009; Tsuchimochi et al., 2013) and cisplatin-induced peripheral neuropathy (Garcia et al., 2008). Our results showed that ghrelin administration lowered ATF3 expression and prevented loss of intraepidermal nerve fibers rather than large sciatic nerves,

suggesting that ghrelin ameliorated the neuropathy in this experimental model by protecting against intraepidermal nerve fiber injuries caused by paclitaxel.

Paclitaxel affects mitochondria in the neurons by opening mitochondrial permeability transition pores and increasing reactive oxygen species production (Bernardi et al., 2006), thus leading to peripheral nerve neuropathy (Duggett et al., 2016). Indeed, levels of markers of oxidative and nitrosative stress, specifically 8-isoprostane, malondialdehyde, and nitric oxide, were increased in our experiment. Ghrelin was shown to reduce oxidative and nitrosative stress in diabetic neuropathy (Kyoraku et al., 2009; Tsuchimochi et al., 2013), sepsis-associated lung injury (Zeng et al., 2015), and nonalcoholic fatty liver disease (Li et al., 2013), supporting our finding that ghrelin exerted a neuroprotective effect against paclitaxel-induced neuropathy. Ghrelin reduces the production of oxidative stress in the mitochondria of neurons by increasing the expression of UCP2 (Andrews et al., 2008). Ghrelin also increases mitochondrial proliferation by inducing UCP2 and activating PGC-1α (Wu et al., 1999; Andrews et al., 2008; Fujimura et al., 2014). Moreover, ghrelin increases the expression of mitochondrial SOD2, leading to decreased oxidative and nitrosative stress (Xu et al., 2008; Dobutovic et al., 2014).

These mechanisms underlying ghrelin's effect on oxidative stress have been reported

306 in several pathologic conditions, such as an 1-methyl-4-phenyl-1, 2, 3, 6-tetrahydropyridine
307 (MPTP)-induced Parkinson's disease experimental model (Andrews et al., 2009), traumatic
308 brain injury (Lopez et al., 2012), hemorrhagic shock (Qi et al., 2014), and a renal fibrosis model
309 (Fujimura et al., 2014). In the setting of peripheral neuropathy, this is the first study to
310 demonstrate that ghrelin reduced oxidative and nitrosative stress in dorsal root ganglia neurons
311 by inducing UCP2, PGC-1α, and SOD2. Taken together, the above findings suggest that ghrelin
312 exerts a neuroprotective effect by improving mitochondrial anti-oxidant functions. Paclitaxel-
313 induced neuropathy involves multiple mechanisms in addition to oxidative stress, including
314 inflammation, intracellular Ca^{2+} dysfunction, ion channel dysfunction, and transient potential
315 receptor activation (reviewed in (Carozzi et al., 2015)). Further studies are needed to elucidate
316 the molecular mechanisms of ghrelin's effect on paclitaxel-induced neuropathy.
317
318 Previous studies also showed that ghrelin-null mice and growth hormone secretagogue
319 receptor-null mice developed more serious pathology in some experimental models; for
320 example, growth hormone secretagogue receptor-null mice were injured more severely in a
321 renal fibrosis model (Fujimura et al., 2014) and a hepatic ischemia model (Qin et al., 2014) than
322 WT mice. We here confirmed that growth hormone secretagogue receptor was expressed in the
323 dorsal root ganglia neurons of growth hormone secretagogue receptor-eGFP mice. Erriquez et

al. (2009) demonstrated that neurons in embryonic chick dorsal root ganglia expressed growth hormone secretagogue receptor and that ghrelin partially increased neuronal cytosolic calcium concentrations. Endogenous ghrelin possibly exerted a direct neuroprotective effect on peripheral neurons through interactions with growth hormone secretagogue receptor, and attenuated paclitaxel-induced neuropathy through ghrelin/ growth hormone secretagogue receptor signaling.

In conclusion, we demonstrated that ghrelin ameliorated paclitaxel-induced neuropathy by preventing intraepidermal nerve fiber injuries. The mechanisms of ghrelin's neuroprotective effect involved suppressing oxidative stress by activating mitochondrial anti-oxidant functions through induction of UCP2 and SOD2, and by increasing mitochondrial numbers. In addition, endogenous ghrelin exerted neuroprotective effects through its interaction with growth hormone secretagogue receptor; this would then directly affect peripheral neurons via this receptor's signaling. The pleiotropic effects of ghrelin against paclitaxel-induced neuropathy that were demonstrated in this study suggest a novel and attractive therapeutic strategy for the prevention of neuropathy during paclitaxel treatment in humans.

Reference

Andrews, Z.B., Diano, S., Horvath, T.L., 2005. Mitochondrial uncoupling proteins in the CNS: in support of function and survival. Nat Rev Neurosci 6, 829-840.

Andrews, Z.B., Erion, D., Beiler, R., Liu, Z.W., Abizaid, A., Zigman, J., Elsworth, J.D., Savitt, J.M., DiMarchi, R., Tschoep, M., Roth, R.H., Gao, X.B., Horvath, T.L., 2009. Ghrelin promotes and protects nigrostriatal dopamine function via a UCP2-dependent mitochondrial mechanism. J Neurosci 29, 14057-14065.

Andrews, Z.B., Liu, Z.W., Walllingford, N., Erion, D.M., Borok, E., Friedman, J.M., Tschop, M.H., Shanabrough, M., Cline, G., Shulman, G.I., Coppola, A., Gao, X.B., Horvath, T.L., Diano, S., 2008. UCP2 mediates ghrelin's action on NPY/AgRP neurons by lowering free radicals. Nature 454, 846-851.

Bernardi, P., Krauskopf, A., Basso, E., Petronilli, V., Blachly-Dyson, E., Di Lisa, F., Forte, M.A., 2006. The mitochondrial permeability transition from in vitro artifact to disease target. Febs j 273, 2077-2099.

Bobylev, I., Joshi, A.R., Barham, M., Ritter, C., Neiss, W.F., Hoke, A., Lehmann, H.C., 2015. Paclitaxel inhibits mRNA transport in axons. Neurobiol Dis 82, 321-331.

Boyette-Davis, J., Xin, W., Zhang, H., Dougherty, P.M., 2011. Intraepidermal nerve fiber loss corresponds to the development of taxol-induced hyperalgesia and can be prevented by

360 treatment with minocycline. Pain 152, 308-313.

361 Carozzi, V.A., Canta, A., Chiorazzi, A., 2015. Chemotherapy-induced peripheral neuropathy:

362 What do we know about mechanisms? Neurosci Lett 596, 90-107.

363 Chaplan, S.R., Bach, F.W., Pogrel, J.W., Chung, J.M., Yaksh, T.L., 1994. Quantitative

364 assessment of tactile allodynia in the rat paw. J Neurosci Methods 53, 55-63.

365 Dobutovic, B., Sudar, E., Tepavcevic, S., Djordjevic, J., Djordjevic, A., Radojcic, M., Isenovic,

366 E.R., 2014. Effects of ghrelin on protein expression of antioxidative enzymes and iNOS in the

367 rat liver. Arch Med Sci 10, 806-816.

368 Duggett, N.A., Griffiths, L.A., McKenna, O.E., de Santis, V., Yongsanguanchai, N., Mokori,

369 E.B., Flatters, S.J., 2016. Oxidative stress in the development, maintenance and resolution of

370 paclitaxel-induced painful neuropathy. Neuroscience 333, 13-26.

371 Erriquez, J., Bernascone, S., Ciarletta, M., Filigheddu, N., Graziani, A., Distasi, C., 2009.

372 Calcium signals activated by ghrelin and D-Lys(3)-GHRP-6 ghrelin antagonist in developing

373 dorsal root ganglion glial cells. Cell Calcium 46, 197-208.

374 Fujimura, K., Wakino, S., Minakuchi, H., Hasegawa, K., Hosoya, K., Komatsu, M., Kaneko, Y.,

375 Shinozuka, K., Washida, N., Kanda, T., Tokuyama, H., Hayashi, K., Itoh, H., 2014. Ghrelin

376 protects against renal damages induced by angiotensin-II via an antioxidative stress mechanism

377 in mice. PLoS One 9, e94373.

Garcia, J.M., Cata, J.P., Dougherty, P.M., Smith, R.G., 2008. Ghrelin prevents cisplatin-induced mechanical hyperalgesia and cachexia. Endocrinology 149, 455-460.

Giuliani, D., Bitto, A., Galantucci, M., Zaffe, D., Ottani, A., Irrera, N., Neri, L., Cavallini, G.M., Altavilla, D., Botticelli, A.R., Squadrito, F., Guarini, S., 2014. Melanocortins protect against progression of Alzheimer's disease in triple-transgenic mice by targeting multiple pathophysiological pathways. Neurobiol Aging 35, 537-547.

Kawai, S., Takagi, Y., Kaneko, S., Kurosawa, T., 2011. Effect of three types of mixed anesthetic agents alternate to ketamine in mice. Exp Anim 60, 481-487.

Ko, M.H., Chen, W.P., Hsieh, S.T., 2002. Neuropathology of skin denervation in acrylamide-induced neuropathy. Neurobiol Dis 11, 155-165.

Ko, M.H., Hu, M.E., Hsieh, Y.L., Lan, C.T., Tseng, T.J., 2014. Peptidergic intraepidermal nerve fibers in the skin contribute to the neuropathic pain in paclitaxel-induced peripheral neuropathy. Neuropeptides 48, 109-117.

Kojima, M., Hosoda, H., Date, Y., Nakazato, M., Matsuo, H., Kangawa, K., 1999. Ghrelin is a growth-hormone-releasing acylated peptide from stomach. Nature 402, 656-660.

Kojima, M., Kangawa, K., 2006. Drug insight: The functions of ghrelin and its potential as a multitherapeutic hormone. Nat Clin Pract Endocrinol Metab 2, 80-88.

Konaka, K., Moriyama, K., Sakurada, T., Okada, N., Imanishi, M., Zamami, Y., Kawazoe, K.,

396 Fushitani, S., Ishizawa, K., 2017. Kamishoyosan and Shakuyakukanzoto promote recovery from
397 paclitaxel-induced neurite retraction in PC12 cells. J Pharm Health Care Sci 3, 20.
398 Kyoraku, I., Shiomi, K., Kangawa, K., Nakazato, M., 2009. Ghrelin reverses experimental
399 diabetic neuropathy in mice. Biochem Biophys Res Commun 389, 405-408.
400 Li, Y., Hai, J., Li, L., Chen, X., Peng, H., Cao, M., Zhang, Q., 2013. Administration of ghrelin
401 improves inflammation, oxidative stress, and apoptosis during and after non-alcoholic fatty liver
402 disease development. Endocrine 43, 376-386.
403 Liu, X., Xiao, Q., Zhao, K., Gao, Y., 2013. Ghrelin inhibits high glucose-induced PC12 cell
404 apoptosis by regulating TLR4/NF-kappaB pathway. Inflammation 36, 1286-1294.
405 Lopez, N.E., Gaston, L., Lopez, K.R., Coimbra, R.C., Hageny, A., Putnam, J., Eliceiri, B.,
406 Coimbra, R., Bansal, V., 2012. Early ghrelin treatment attenuates disruption of the blood brain
407 barrier and apoptosis after traumatic brain injury through a UCP-2 mechanism. Brain Res 1489,
408 140-148.
409 Masocha, W., 2014. Paclitaxel-induced hyposensitivity to nociceptive chemical stimulation in
410 mice can be prevented by treatment with minocycline. Sci Rep 4, 6719.
411 Masocha, W., Kombian, S.B., Edafiogho, I.O., 2016. Evaluation of the antinociceptive activities
412 of enaminone compounds on the formalin and hot plate tests in mice. Sci Rep 6, 21582.
413 Nakazato, M., Murakami, N., Date, Y., Kojima, M., Matsuo, H., Kangawa, K., Matsukura, S.,

414 2001. A role for ghrelin in the central regulation of feeding. Nature 409, 194-198.

415 Polomano, R.C., Mannes, A.J., Clark, U.S., Bennett, G.J., 2001. A painful peripheral neuropathy

416 in the rat produced by the chemotherapeutic drug, paclitaxel. Pain 94, 293-304.

417 Qi, L., Cui, X., Dong, W., Barrera, R., Coppa, G.F., Wang, P., Wu, R., 2014. Ghrelin protects

418 rats against traumatic brain injury and hemorrhagic shock through upregulation of UCP2. Ann

419 Surg 260, 169-178.

420 Qin, Y., Li, Z., Wang, Z., Li, Y., Zhao, J., Mulholland, M., Zhang, W., 2014. Ghrelin contributes

421 to protection of hepatocellular injury induced by ischaemia/reperfusion. Liver Int 34, 567-575.

422 Rowinsky, E.K., Donehower, R.C., 1995. Paclitaxel (taxol). N Engl J Med 332, 1004-1014.

423 Sato, T., Kurokawa, M., Nakashima, Y., Ida, T., Takahashi, T., Fukue, Y., Ikawa, M., Okabe, M.,

424 Kangawa, K., Kojima, M., 2008. Ghrelin deficiency does not influence feeding performance.

425 Regul Pept 145, 7-11.

426 Sommer, C., Schafers, M., 1998. Painful mononeuropathy in C57BL/Wld mice with delayed

427 wallerian degeneration: differential effects of cytokine production and nerve regeneration on

428 thermal and mechanical hypersensitivity. Brain Res 784, 154-162.

429 Sun, Y., Wang, P., Zheng, H., Smith, R.G., 2004. Ghrelin stimulation of growth hormone release

430 and appetite is mediated through the growth hormone secretagogue receptor. Proc Natl Acad Sci

431 U S A 101, 4679-4684.

Tofthagen, C., 2010. Patient perceptions associated with chemotherapy-induced peripheral neuropathy. Clin J Oncol Nurs 14, E22-28.

Tsuchimochi, W., Kyoraku, I., Yamaguchi, H., Toshinai, K., Shiomi, K., Kangawa, K., Nakazato, M., 2013. Ghrelin prevents the development of experimental diabetic neuropathy in rodents. Eur J Pharmacol 702, 187-193.

Tsujino, H., Kondo, E., Fukuoka, T., Dai, Y., Tokunaga, A., Miki, K., Yonenobu, K., Ochi, T., Noguchi, K., 2000. Activating transcription factor 3 (ATF3) induction by axotomy in sensory and motoneurons: A novel neuronal marker of nerve injury. Mol Cell Neurosci 15, 170-182.

Wu, Z., Puigserver, P., Andersson, U., Zhang, C., Adelmant, G., Mootha, V., Troy, A., Cinti, S., Lowell, B., Scarpulla, R.C., Spiegelman, B.M., 1999. Mechanisms controlling mitochondrial biogenesis and respiration through the thermogenic coactivator PGC-1. Cell 98, 115-124.

Xu, Z., Lin, S., Wu, W., Tan, H., Wang, Z., Cheng, C., Lu, L., Zhang, X., 2008. Ghrelin prevents doxorubicin-induced cardiotoxicity through TNF-alpha/NF-kappaB pathways and mitochondrial protective mechanisms. Toxicology 247, 133-138.

Zeng, M., He, W., Li, L., Li, B., Luo, L., Huang, X., Guan, K., Chen, W., 2015. Ghrelin attenuates sepsis-associated acute lung injury oxidative stress in rats. Inflammation 38, 683-690.

Zhang, H., Boyette-Davis, J.A., Kosturakis, A.K., Li, Y., Yoon, S.Y., Walters, E.T., Dougherty, P.M., 2013. Induction of monocyte chemoattractant protein-1 (MCP-1) and its receptor CCR2 in

primary sensory neurons contributes to paclitaxel-induced peripheral neuropathy. J Pain 14, 1031-1044.

Zhang, H., Li, Y., de Carvalho-Barbosa, M., Kavelaars, A., Heijnen, C.J., Albrecht, P.J., Dougherty, P.M., 2016. Dorsal Root Ganglion Infiltration by Macrophages Contributes to Paclitaxel Chemotherapy-Induced Peripheral Neuropathy. J Pain 17, 775-786.

458 **Figure legends**

459

460 **Fig. 1.** Effects of ghrelin administration on mechanical and thermal hypersensitivity and body
461 weight. (A) Mechanical withdrawal threshold was measured by the von Frey test (n = 9–10) on
462 Day 1 and Day 7; (B) thermal withdrawal threshold was evaluated by the hot plate test (n = 10–
463 11) on Day 1 and Day 7; (C) body weight on Day 1 and Day 7. (D) Immunohistochemistry for
464 anti-GFP antibodies in dorsal root ganglia of growth hormone secretagogue receptor-enhanced
465 green fluorescent protein mice. Scale bars: 20 μm. Values are means ± S.E.M. **P* < 0.05, ***P* <
466 0.01. PTX, paclitaxel; GHSR, growth hormone secretagogue receptor; eGFP, enhanced green
467 fluorescent protein.

468

469 **Fig. 2.** Histological analysis of ghrelin's effects on the dorsal root ganglia, sciatic nerve, and
470 intraepidermal nerve fibers. (A) Immunohistochemical detection of ATF3 in the dorsal root
471 ganglia and (B) ratio of ATF3-positive cells in NeuN-positive cells (n = 5). Scale bars: 100 μm.
472 (C) Representative micrographs of sciatic nerves and (D) histograms of myelinated axon
473 diameter (n = 7–8). Scale bars: 20 μm. (E) Representative immunohistochemical staining for
474 PGP9.5 and (F) the density of intraepidermal nerve fibers in hind paw skin (n = 6). Dotted line
475 shows the border between epidermis and dermis. Scale bars: 50 μm. Values are means ± S.E.M.

476 *$P < 0.05$, **$P < 0.01$. PTX, paclitaxel; IENF, intraepidermal nerve fiber.

477

478 **Fig. 3.** Effects of ghrelin on systemic oxidative and nitrosative stress, and mitochondrial anti-
479 oxidant function in dorsal root ganglia. Plasma levels of (A) 8-isoprostane (n = 9), (B)
480 malondialdehyde (n = 9), and (C) nitric oxide (n = 9) were measured on Day 7. (D) The mRNA
481 expression levels of *Ucp2*, *Pgc-1α*, and *Sod2* in the dorsal root ganglia were measured on Day 7
482 (n = 8–9). The mRNA levels were normalized against *Gapdh* mRNA levels, and shown relative
483 to the control group. (E) Representative images of immunocytochemical staining of SOD2 and
484 the SOD2 fluorescent intensity in PC12 cells (n = 4). Scale bar: 5 μm. (F) Representative
485 images and analysis of a western blot of SOD2 in PC12 cells (n = 4). β-actin was used as a
486 loading control. Values are means ± S.E.M. *$P < 0.05$, **$P < 0.01$. PTX, paclitaxel.

487

488 **Fig. 4.** Effects of endogenous ghrelin on paclitaxel-induced nerve injuries in ghrelin-null and
489 growth hormone secretagogue receptor-null mice, and histological evaluation of growth
490 hormone secretagogue receptor in peripheral neurons in growth hormone secretagogue receptor-
491 eGFP mice. (A) Mechanical withdrawal threshold was measured by the von Frey test (n = 6).
492 (B) Immunohistochemical detection of ATF3 in dorsal root ganglia and ratio of the ATF3-
493 positive cells in NeuN-positive cells (n = 6–7). Scale bars: 100 μm. Values are means ± S.E.M.

494 *$P < 0.05$, **$P < 0.01$. PTX, paclitaxel; GHSR, growth hormone secretagogue receptor.

495

Figure 1

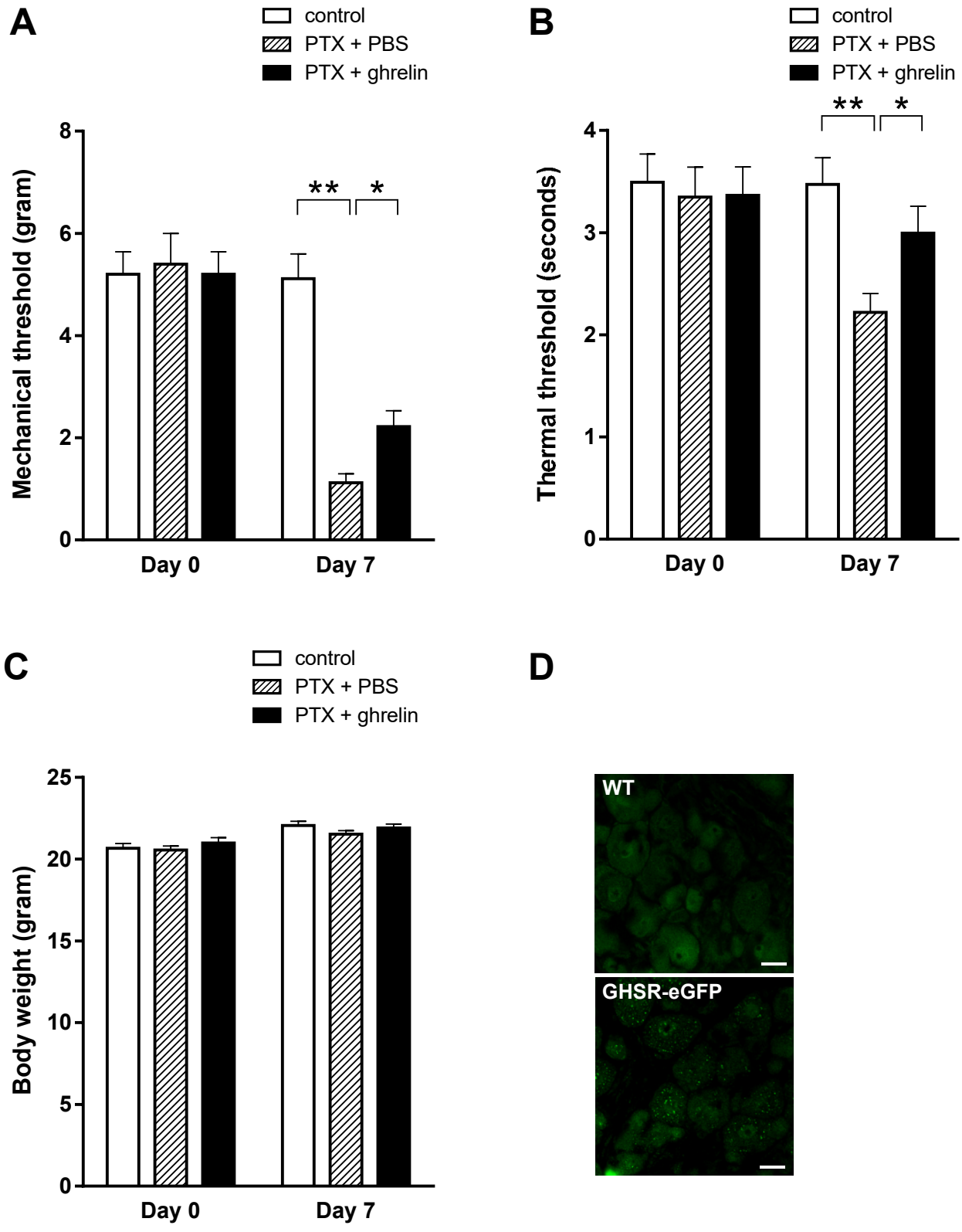
A
control
PTX + PBS
PTX + ghrelin
Mechanical threshold (gram)
8
6
4
2
0
**
*
Day 0
Day 7
B
control
PTX + PBS
PTX + ghrelin
Thermal threshold (seconds)
4
3
2
1
0
**
*
Day 0
Day 7
C
control
PTX + PBS
PTX + ghrelin
Body weight (gram)
25
20
15
10
5
0
Day 0
Day 7
D
WT
GHSR-eGFP

Figure 2

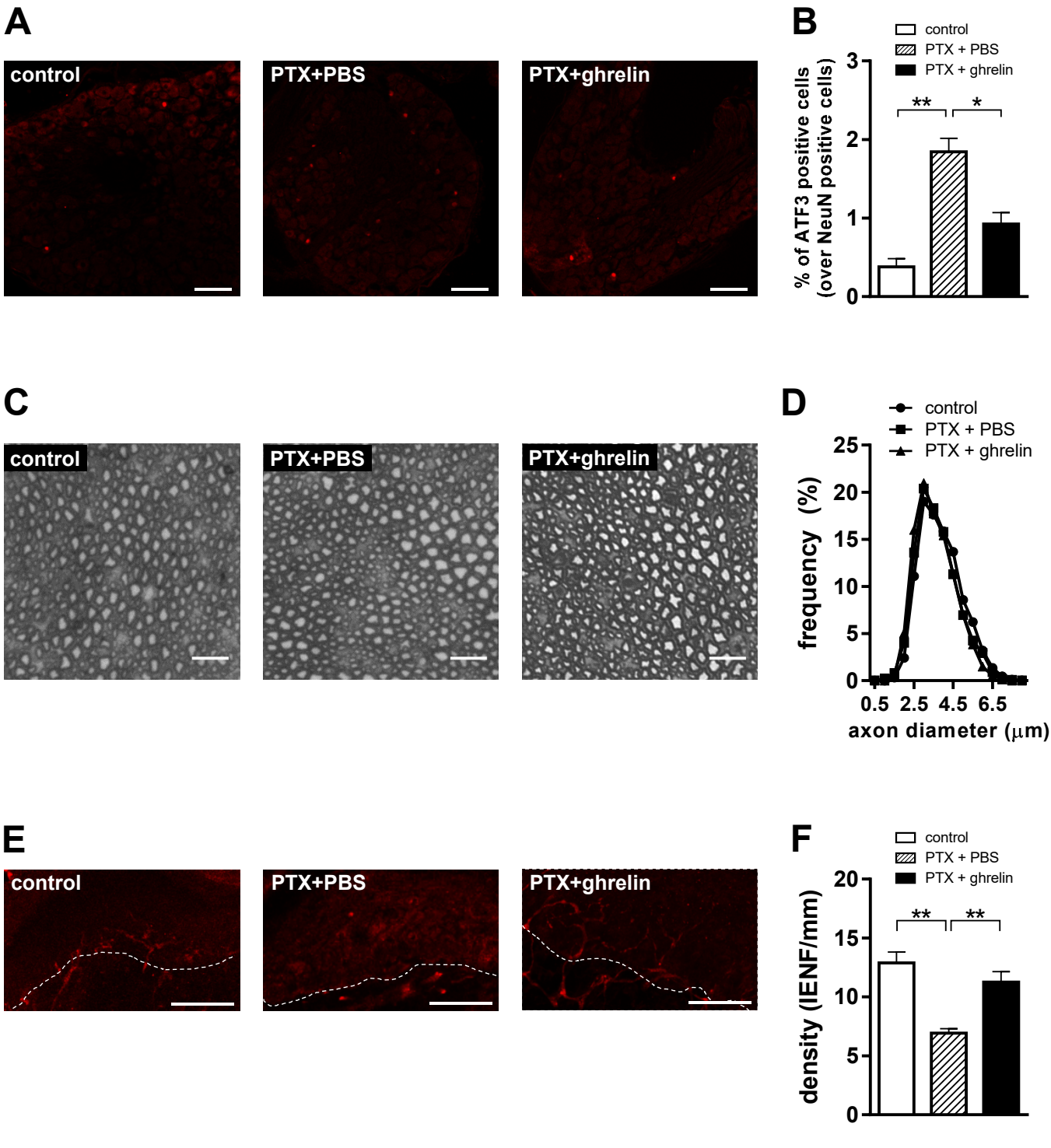
A
control
PTX+PBS
PTX+ghrelin
B
control
PTX + PBS
PTX + ghrelin
% of ATF3 positive cells (over NeuN positive cells)
0
1
2
3
**
*
C
control
PTX+PBS
PTX+ghrelin
D
control
PTX + PBS
PTX + ghrelin
frequency (%)
0
5
10
15
20
25
0.5 2.5 4.5 6.5
axon diameter (μm)
E
control
PTX+PBS
PTX+ghrelin
F
control
PTX + PBS
PTX + ghrelin
density (IENF/mm)
0
5
10
15
20
**
**

Figure 3

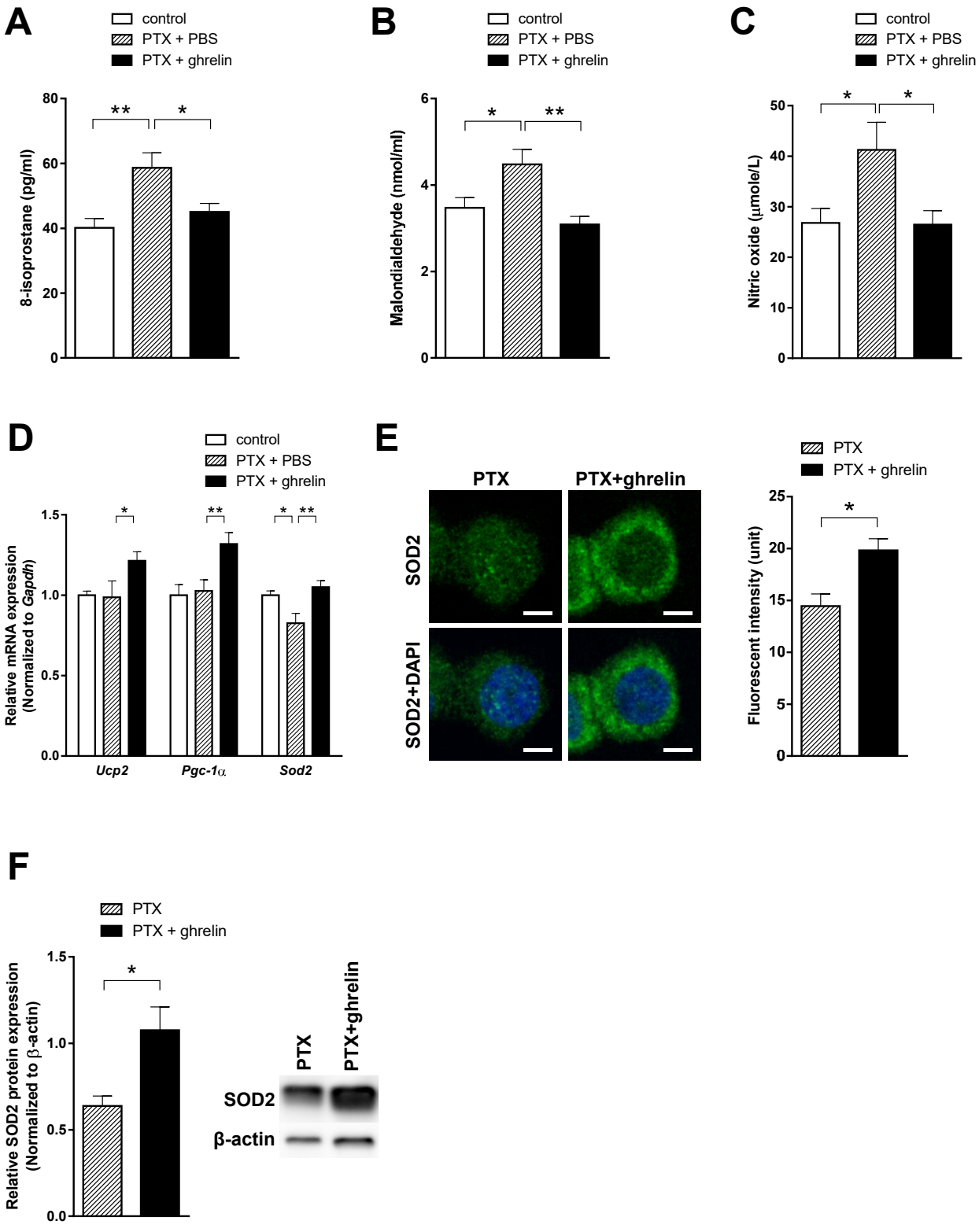
A
control
PTX + PBS
PTX + ghrelin
8-isoprostane (pg/ml)
B
Malondialdehyde (nmol/ml)
C
Nitric oxide (μmole/L)
D
Relative mRNA expression (Normalized to Gapdh)
Ucp2
Pgc-1α
Sod2
E
PTX
PTX+ghrelin
SOD2
SOD2+DAPI
Fluorescent intensity (unit)
F
Relative SOD2 protein expression (Normalized to β-actin)
SOD2
β-actin

Figure 4

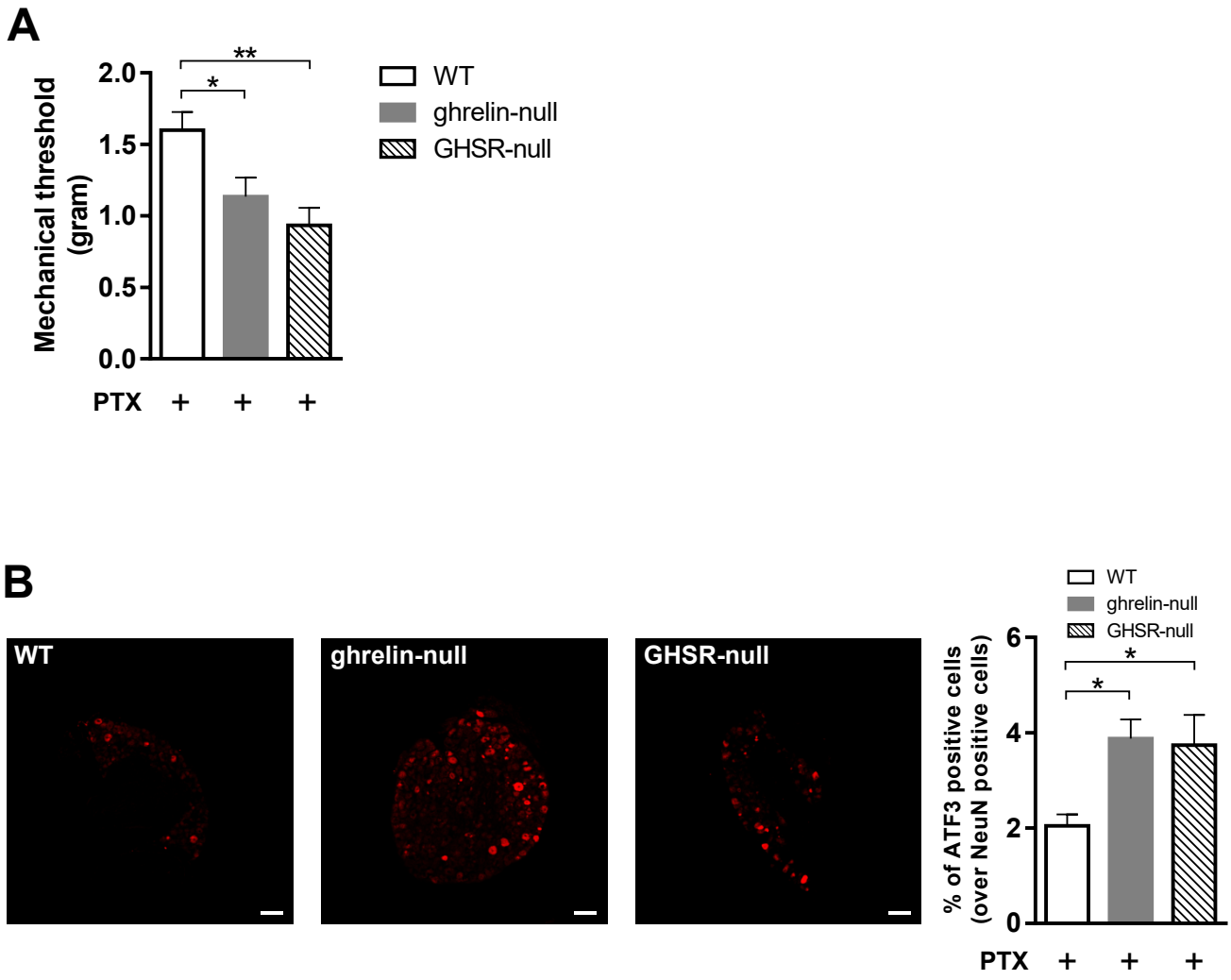
A
Mechanical threshold (gram)
2.0
1.5
1.0
0.5
0.0
**
*
WT
ghrelin-null
GHSR-null
PTX + + +
B
WT
ghrelin-null
GHSR-null
% of ATF3 positive cells (over NeuN positive cells)
6
4
2
0
*
*
PTX + + +